



# Quantum Electrodynamics and Quantum Optics: Lecture 12

Fall 2025

## Quantum measurements and measurement back-action

Free-particle Hamiltonian:  $\hat{H}_0 = \frac{\hat{p}^2}{2m}$ .

First measurement at time  $t = 0$ , yields  $\hat{x}(0)$  and  $\hat{p}(0)$ . Variances of these quantities  $\Delta\hat{x}^2 = \langle\hat{x}^2\rangle - \langle\hat{x}\rangle^2$  follow Heisenberg uncertainty:

$$\Delta\hat{p}(0)\Delta\hat{x}(0) \geq \frac{\hbar}{2}$$

Time-evolution for small time  $\tau$ :

$$\frac{d\hat{x}}{dt} = -\frac{i}{\hbar}[\hat{x}, \hat{H}] = \hat{p}/m \implies \hat{x}(\tau) = \hat{x}(0) + \frac{\hat{p}(0)\tau}{m}$$

Measurement at time  $\tau$  will have the uncertainty:

$$\Delta\hat{x}(\tau)^2 = \Delta\hat{x}(0)^2 + \frac{\Delta\hat{p}(0)^2\tau^2}{m^2} + (\langle\hat{x}(0)\hat{p}(0) + \hat{p}(0)\hat{x}(0)\rangle - 2\langle\hat{p}(0)\rangle\langle\hat{x}(0)\rangle) \frac{\tau}{m}$$

## Quantum measurements and measurement back-action

Assume that position and momentum are not correlated. Thus we have for the uncertainty at time  $\tau$ :

$$\Delta\hat{x}(\tau)^2 = \Delta\hat{x}(0)^2 + \frac{\hbar^2\tau^2}{4m^2\Delta\hat{x}(0)^2}.$$

First measurement at  $t = 0$  introduces an uncertainty for the second measurement at  $t = \tau$ . This is referred to as the *measurement back-action*. The minimum possible uncertainty due to measurement back-action is called the *standard quantum limit* (SQL)

### Standard Quantum Limit (SQL)

$$\Delta\hat{x}(\tau)^2 = \frac{\hbar\tau}{m}$$

Consider the case of gravitational wave detection<sup>1</sup>, where  $\tau \sim 1$  ms and  $m = 4$  kg. These parameters give  $\Delta\hat{x}(\tau)_{SQL} \sim 10^{-18}$  m.

<sup>1</sup>Ref. Ch. 14 *Quantum Optics* GJ Milburn, DF Walls

## Harmonic oscillator quantum limit

Consider harmonic oscillator Hamiltonian:  $\hat{H}_0 = \frac{\hat{p}^2}{2m} + \frac{m\Omega_m^2 \hat{x}^2}{2}$ , the dynamics follows

$$\hat{x}(\tau) = \hat{x}(0) \cos(\Omega_m \tau) + \frac{\hat{p}(0)}{m\Omega_m} \sin(\Omega_m \tau)$$

$$[\hat{x}(0), \hat{x}(\tau)] = \frac{i\hbar}{m\Omega_m} \sin(\Omega_m \tau), \quad \Delta\hat{x}(0)^2 \Delta\hat{p}(0)^2 \geq \frac{\hbar^2}{4}.$$

When measuring at a later time, at half-period (when  $\Omega_m \tau = \pi/2$ ):

### Limit for periodic measurement

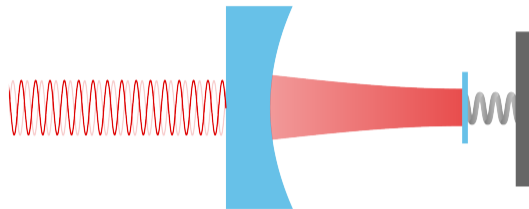
$$\sqrt{\Delta\hat{x}(\tau)^2} \geq \sqrt{\frac{\hbar}{2m\Omega_m}} \equiv \text{zero-point motion}$$

Velocity and position cannot be determined simultaneously due to the uncertainty principle.

## Optomechanics

*Dispersive coupling* of the mass to the cavity field:

$$\begin{aligned}\omega_{c,m} &= m \frac{c\pi}{L} \\ \omega_{c,m}(x) &= m \frac{c\pi}{L+x} \\ &= \omega_{c,m} \left(1 - \frac{x}{L}\right).\end{aligned}$$



We consider the fundamental mode that  $m = 1$ . Hamiltonian of the mass-cavity system is thus modified:

$$\hat{H} = \hbar\omega_c \left(1 - \frac{\hat{x}}{L}\right) \hat{a}^\dagger \hat{a} + \hbar\Omega_m \hat{b}^\dagger \hat{b}.$$

The interaction part of the Hamiltonian arises from the changing cavity frequency:

$$\hat{H}_{\text{int}} = -\hbar \frac{\omega_c}{L} x_{\text{zpf}} \hat{a}^\dagger \hat{a} (\hat{b} + \hat{b}^\dagger).$$

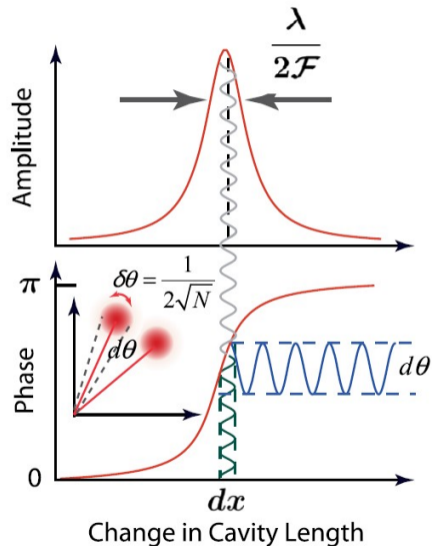
# Optomechanics

Reflection from the cavity at resonance  
( $\omega = \omega_c$ ):

$$\begin{aligned} r[\omega] &= \frac{\omega - \omega_c(x) - i\kappa/2}{\omega - \omega_c(x) + i\kappa/2} \\ &= \frac{\omega_c x/L - i\kappa/2}{\omega_c x/L + i\kappa/2} \end{aligned}$$

Phase shift around resonance of the reflected field

$$\theta \sim 2 \frac{x}{L} \frac{\omega_c}{\hbar} \propto x$$



## Quantum Langevin equations

Recall: Coupling between system and bath

$$\hat{H}_B = \int d\omega \hbar\omega \hat{b}^\dagger[\omega] \hat{b}[\omega] \quad \text{and} \quad \hat{H}_{SB} = \int d\omega \hbar g[\omega] \left( \hat{a} \hat{b}^\dagger[\omega] + \hat{a}^\dagger \hat{b}[\omega] \right).$$

Time-evolution of the operators in the Heisenberg picture includes a dissipation term and a fluctuation term:

$$\frac{d\hat{a}}{dt} = -\frac{i}{\hbar} [\hat{a}, \hat{H}_{\text{sys}}] - \frac{\kappa}{2} \hat{a} + \sqrt{\kappa} \hat{a}_{\text{in}}.$$

For the optomechanical Hamiltonian,  $\hat{H} = \hbar\omega_c \left( 1 - \frac{\hat{x}}{L} \right) \hat{a}^\dagger \hat{a} + \hbar\Omega_m \hat{b}^\dagger \hat{b}$ , we get the following equations of motion with drive:

$$\begin{aligned} \frac{d\hat{a}}{dt} &= -i\omega_c \hat{a} + i\frac{\omega_c}{L} x_{\text{zpf}} \hat{a} \left( \hat{b} + \hat{b}^\dagger \right) - \frac{\kappa}{2} \hat{a} + \sqrt{\kappa} (\hat{a}_{\text{in}} + \bar{a}_{\text{in}} e^{i\omega_L t}), \\ \frac{d\hat{b}}{dt} &= -i\Omega_m \hat{b} + i\frac{\omega_c}{L} x_{\text{zpf}} \hat{a}^\dagger \hat{a} - \frac{\Gamma_m}{2} \hat{b} + \sqrt{\Gamma_m} \hat{b}_{\text{in}}. \end{aligned}$$

## Quantum Langevin equations

We transfer to a rotating frame,  $\hat{a} \rightarrow \hat{a}e^{i\omega_L t}$ . We consider the case when the cavity is resonantly driven, i.e.  $\omega_L = \omega_c$ . Next we assume that the fields are strong, so they can be represented as a sum of a mean value and small fluctuations:

$$\hat{a} \rightarrow \bar{\alpha} + \delta\hat{a} \quad \text{and} \quad \hat{b} \rightarrow \bar{\beta} + \delta\hat{b}.$$

The interaction Hamiltonian  $\hat{H}_{\text{int}} = \hbar \frac{\omega_c}{L} x_{\text{zpf}} \hat{a}^\dagger \hat{a} (\hat{b}^\dagger + \hat{b})$  is thus *linearized*:

$$\hat{a}^\dagger \hat{a} = (\bar{\alpha}^* + \delta\hat{a}^\dagger)(\bar{\alpha} + \delta\hat{a}) \rightarrow \bar{\alpha} (\delta\hat{a} + \delta\hat{a}^\dagger)$$

Redefining  $\delta\hat{a}$  as  $\hat{a}$ , we get *linearized quantum Langevin equations*:

$$\begin{aligned} \frac{d\hat{a}}{dt} &= i \frac{\omega_c}{L} x_{\text{zpf}} \bar{\alpha} (\hat{b} + \hat{b}^\dagger) - \frac{\kappa}{2} \hat{a} + \sqrt{\kappa} \hat{a}_{\text{in}}, \\ \frac{d\hat{b}}{dt} &= -i\Omega_m \hat{b} + i \frac{\omega_c}{L} \bar{\alpha} (\hat{a} + \hat{a}^\dagger) - \frac{\Gamma_m}{2} \hat{b} + \sqrt{\Gamma_m} \hat{b}_{\text{in}}. \end{aligned}$$

## Quadratures

Next we consider the fluctuations in amplitude and phase quadratures:

$$\hat{X} \equiv \frac{1}{\sqrt{2}} (\hat{a} + \hat{a}^\dagger) \quad \text{and} \quad \hat{Y} \equiv \frac{i}{\sqrt{2}} (\hat{a}^\dagger - \hat{a}).$$

The Langevin equations for the optical field can be expressed as

$$\begin{aligned} \frac{d\hat{X}}{dt} &= -\frac{\kappa}{2}\hat{X} + \sqrt{\kappa}\hat{X}_{\text{in}} \\ \frac{d\hat{Y}}{dt} &= i\sqrt{2}x_{\text{zpf}}\frac{\omega_c}{L}\bar{\alpha}(\hat{b} + \hat{b}^\dagger) - \frac{\kappa}{2}\hat{Y} + \sqrt{\kappa}\hat{Y}_{\text{in}} \end{aligned}$$

Position of the mechanical oscillator is only imprinted on the phase of the optical field  
 $\implies$  We can infer position using *homodyne detection*.

## Input-output relations

The input-output relation for fields also applies to the quadratures:

$$\hat{a}_{\text{out}} = -\hat{a}_{\text{in}} + \sqrt{\kappa}\hat{a} \quad \Longrightarrow \quad \hat{Y}_{\text{out}} = -\hat{Y}_{\text{in}} + \sqrt{\kappa}\hat{Y}.$$

Taking the Fourier transform  $\hat{Y}[\omega] = \int_{-\infty}^{\infty} e^{i\omega t} \hat{Y}(t) dt$ , and redefining  $\hat{q} = \hat{x} = x_{\text{zpf}} (\hat{b} + \hat{b}^\dagger)$  for readability yields

$$-i\omega\hat{Y}[\omega] = i\sqrt{2}\frac{\omega_c}{L}\bar{\alpha}\hat{q}[\omega] - \frac{\kappa}{2}\hat{Y}[\omega] + \sqrt{\kappa}\hat{Y}_{\text{in}}[\omega].$$

After substitution, we assume so-called bad-cavity limit  $\kappa \gg \Omega_m$  and derive the output phase quadrature:

$$\hat{Y}_{\text{out}}[\omega] = \hat{Y}_{\text{in}}[\omega] + i\frac{\bar{\alpha}\omega_c}{L}\sqrt{\frac{8}{\kappa}}\hat{q}[\omega].$$

## Spectral densities

We can find spectral densities by Wiener-Khinchin theorem:

$$\begin{aligned} S_{\hat{Y}\hat{Y}}[\omega] &= \lim_{\tau \rightarrow \infty} \frac{1}{\tau} \langle \hat{Y}_\tau^\dagger[\omega] \hat{Y}_\tau[\omega] \rangle \\ &= \int d\tau e^{-i\omega\tau} \langle \hat{Y}^\dagger(\tau) \hat{Y}(0) \rangle = \int_{-\infty}^{\infty} d\omega' \langle \hat{Y}^\dagger[-\omega] \hat{Y}[\omega'] \rangle \end{aligned}$$

The input noise and mechanical motion are not correlated:  $\langle \hat{Y}_{in}(\omega) \hat{q}(\omega) \rangle = 0$ , and using the relations:

$$\langle \hat{Y}_{in}(t) \hat{Y}_{in}^\dagger(t') \rangle = (\bar{n} + 1) \delta(t - t'), \quad \langle \hat{Y}_{in}^\dagger(t) \hat{Y}_{in}(t') \rangle = \bar{n} \delta(t - t')$$

Spectral density of the output noise is given by

$$S_{\hat{Y}_{out}\hat{Y}_{out}}[\omega] = \underbrace{1}_{\text{Shot noise } S_{\hat{Y}_{in}\hat{Y}_{in}}} + \underbrace{\frac{8\omega_c^2 \bar{\alpha}^2}{\kappa L^2} S_{\hat{q}\hat{q}}[\omega]}_{\text{signal}}$$

## SQL and Heisenberg uncertainty

The weakest signal  $S_{\hat{q}\hat{q}}^{\text{imp}}$  that can be measured is when the signal-to-noise ratio is equal to 1:

$$S_{\hat{q}\hat{q}}^{\text{imp}} = \left( \frac{\kappa L^2}{8\omega_c^2 \bar{\alpha}^2} \right) S_{\hat{Y}_{\text{in}}\hat{Y}_{\text{in}}}$$

Force acting on the mechanical oscillator is  $\hat{F} = -\partial\hat{H}/\partial\hat{q}$ . Assuming  $\dot{\hat{X}} = 0$ ,

$$\hat{F} = \sqrt{2}\hbar\frac{\omega_c}{L}\hat{X} \implies \hat{F} = \sqrt{\frac{8}{\kappa}}\hbar\frac{\omega_c}{L}\hat{X}_{\text{in}}$$

$$\implies S_{\hat{F}\hat{F}}[\omega] = \frac{8}{\kappa} \left( \hbar\frac{\omega_c}{L}\bar{\alpha} \right)^2 S_{\hat{X}_{\text{in}}\hat{X}_{\text{in}}}[\omega]$$

From these two expressions, it can be seen that

$$S_{\hat{F}\hat{F}}[\omega]S_{\hat{q}\hat{q}}^{\text{imp}} = \hbar^2 S_{\hat{Y}_{\text{in}}\hat{Y}_{\text{in}}} S_{\hat{X}_{\text{in}}\hat{X}_{\text{in}}} = \frac{\hbar^2}{4}.$$

## Spectrum of position fluctuations

We write a second order differential equation for position:

$$\ddot{\hat{q}} = -\Omega_m^2 \hat{q} - 2i \frac{\omega_c}{L} \bar{\alpha} x_{\text{zpf}} \hat{X} - \Gamma_m \dot{\hat{q}} + \sqrt{\Gamma_m} \hat{q}_{\text{in}}.$$

Taking the Fourier transform as  $\hat{q}[\omega] = \int_{-\infty}^{\infty} dt e^{i\omega t} \hat{q}(t)$ , we get:

$$\hat{q}[\omega] = \chi[\omega] \left[ -2i \frac{\omega_c}{L} \bar{\alpha} x_{\text{zpf}} \hat{X}[\omega] + \sqrt{\Gamma_m} \hat{q}_{\text{in}} \right],$$

where  $\chi[\omega] = \left( \Omega_m^2 - \omega^2 - i\omega\Gamma_m \right)^{-1}$ .

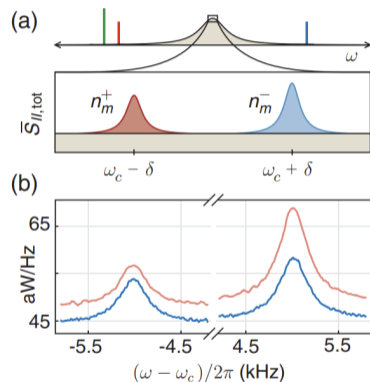
# Noise spectral density

$$S_{\hat{q}\hat{q}}[\omega] = 2\Gamma_m |\chi[\omega]|^2 \left[ S_{\hat{q}_{in}\hat{q}_{in}} + \underbrace{4 \frac{\left(x_{zpf} \bar{\alpha} \frac{\omega_c}{L}\right)^2}{\Gamma_m}}_{C_{eff}} S_{\hat{X}\hat{X}} \right]$$

$$S_{\hat{q}\hat{q}}[\omega] = 2\Gamma_m |\chi[\omega]|^2 (n_{th} + C_{eff} + 1)$$

$$S_{\hat{q}\hat{q}}[-\omega] = 2\Gamma_m |\chi[\omega]|^2 (n_{th} + C_{eff})$$

Asymmetric noise spectral density  $\rightarrow$  In contrast to the classical results!



## Quantum limits in interferometric detection of gravitational radiation

A. F. Pace and M. J. Collett

*Department of Physics, University of Auckland, Private Bag 92019, New Zealand*

D. F. Walls\*

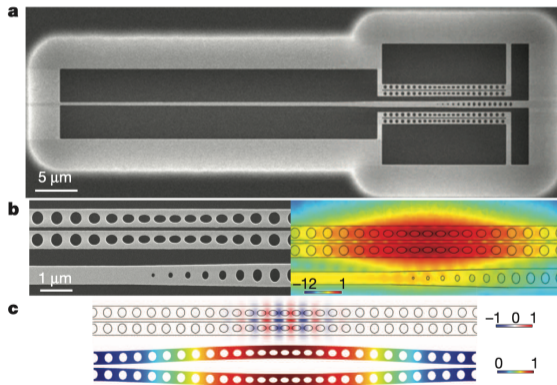
*Joint Institute for Laboratory Astrophysics, University of Colorado, Boulder, Colorado 80309-0440*

(Received 13 July 1992)

A spectral analysis is given of the quantum fluctuations in an optical interferometer to detect gravitational radiation. Two different methods of beating the standard quantum limit are examined: directing a squeezed state into the nonlaser input port of the interferometer and placing a Kerr medium into both arms of the interferometer. For both the Kerr medium and large squeezing cases the interferometer system is limited ultimately by the damping noise in the mirrors, not by noise in the light.

# Squeezed light from a silicon micromechanical resonator

Amir H. Safavi-Naeini<sup>1,2\*</sup>, Simon Gröblacher<sup>1,2\*</sup>, Jeff T. Hill<sup>1,2\*</sup>, Jasper Chan<sup>1</sup>, Markus Aspelmeyer<sup>3</sup> & Oskar Painter<sup>1,2,4</sup>



# Questions

- What is optomechanical Hamiltonian? How does linearization work and how to justify it?
- What is the quantum backaction force on the mechanical oscillator?
- What is the physical mechanism that enables optical squeezing?
- What are the Fourier domain operators? What are their commutation relations and statistical properties?

# Questions

- What is the physically the optical cavity and the mechanical oscillator?
- What is the technical difficulties in observing large optical squeezing?
- How is different optical quadrature spectrum measured?
- What is the typical bandwidth in observing this type of optical squeezing?

# Progressive field-state collapse and quantum non-demolition photon counting

Christine Guerlin<sup>1</sup>, Julien Bernu<sup>1</sup>, Samuel Deléglise<sup>1</sup>, Clément Sayrin<sup>1</sup>, Sébastien Gleyzes<sup>1</sup>, Stefan Kuhr<sup>1,†</sup>, Michel Brune<sup>1</sup>, Jean-Michel Raimond<sup>1</sup> & Serge Haroche<sup>1,2</sup>

The irreversible evolution of a microscopic system under measurement is a central feature of quantum theory. From an initial state generally exhibiting quantum uncertainty in the measured observable, the system is projected into a state in which this observable becomes precisely known. Its value is random, with a probability determined by the initial system's state. The evolution induced by measurement (known as 'state collapse') can be progressive, accumulating the effects of elementary state changes. Here we report the observation of such a step-by-step collapse by non-destructively measuring the photon number of a field stored in a cavity. Atoms behaving as microscopic clocks cross the cavity successively. By measuring the light-induced alterations of the clock rate, information is progressively extracted, until the initially uncertain photon number converges to an integer. The suppression of the photon number spread is demonstrated by correlations between repeated measurements. The procedure illustrates all the postulates of quantum measurement (state collapse, statistical results and repeatability) and should facilitate studies of non-classical fields trapped in cavities.

# An atomic clock to count photons

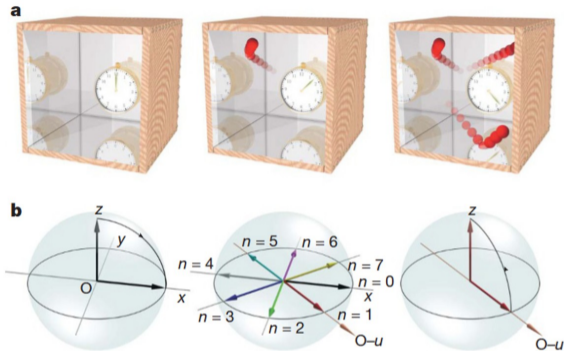


**Figure 1 | Principle of QND photon counting.** **a**, Thought experiment with a clock in a box containing  $n$  photons. The hand of the clock undergoes a  $\pi/4$  phase-advance per photon ( $n = 0, 1, 3$  represented). **b**, Evolution of the atomic spin on the Bloch sphere in a real experiment: an initial pulse  $R_1$  rotates the spin from  $O-z$  to  $O-x$  (left). Light shift produces a  $\pi/4$  phase shift per photon of the spin's precession in the equatorial plane. Directions associated with  $n = 0$  to  $7$  end up regularly distributed over  $360^\circ$  (centre). Pulse  $R_2$  maps the direction  $O-u$  onto  $O-z$ , before the atomic state is read out (right).

The random outcome of a spin detection modifies our knowledge of the photon number distribution. The conditional probability  $P(n|j,\phi)$  for finding  $n$  photons after detecting the spin value  $j$  along  $O-u$  is related to the inverse conditional probability  $P(j,\phi|n)$  by Bayes' law<sup>38</sup>:

$$P(n|j,\phi) = P_0(n)P(j,\phi|n)/P(j,\phi) = P_0(n)[1 + \cos(n\pi/q - \phi + j\pi)]/2P(j,\phi) \quad (1)$$

where  $P(j,\phi) = \sum_n P(j,\phi|n)P_0(n)$  is the a priori probability for  $j$ . This formula directly follows from the definition of conditional probabilities. It can also be derived from the projection postulate<sup>1</sup>. After detection of the spin in state  $|j,\phi\rangle$ , the entangled atom-field system collapses into  $[\sum_n c_n \langle j,\phi|+n\rangle|n\rangle] \otimes |j,\phi\rangle / \sqrt{P(j,\phi)}$ . This entails that the photon number probability is (up to a global factor) multiplied by  $|\langle j,\phi|+n\rangle|^2 = P(j,\phi|n)$ .

# Progressive pinning-down of photon number

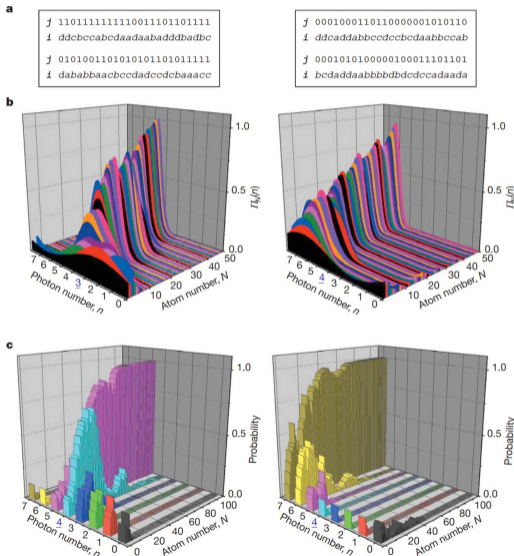


**Figure 2 | Progressive collapse of field into photon number state.**

**a**, Sequences of  $(j, i)$  data (first 50 atoms) produced by two independent measurements.

**b**, Evolution of  $I_N(n)$  for the two sequences displayed in **a**, when  $N$  increases from 1 to 50,  $n$  being treated as a continuous variable (integral of  $I_N(n)$  normalized to unity).

**c**, Photon number probabilities plotted versus photon number and atom numbers  $n$  and  $N$ . The histograms evolve, as  $N$  increases from 0 to 110, from a flat distribution into  $n = 5$  and  $n = 7$  peaks.

In order to obtain more information, we repeat the process and send a sequence of atoms across C. This results in a step-by-step change of the photon number distribution. From one atom to the next, we vary  $\phi$ . Calling  $\phi(k)$  the detection angle for the  $k$ th atom and  $j(k)$  its spin reading, the photon number distribution after  $N$  atoms becomes:

$$P_N(n) = \frac{P_0(n)}{Z} \prod_{k=1}^N [A + B \cos(n\Phi - \phi(k) + j(k)\pi)] \quad (2)$$

where  $Z$  enforces normalization. For an efficient decimation, we alternate between detection directions nearly coinciding with the vectors associated with  $q$  non-orthogonal  $|+_p\rangle$  states. Each atom has a chance to reduce the probability of a photon number different from the one decimated by its predecessor. After a finite number of steps, numerical simulations predict that a single  $n$  value (modulo  $2q$ ) survives.

# Reconstructing photon number statistics

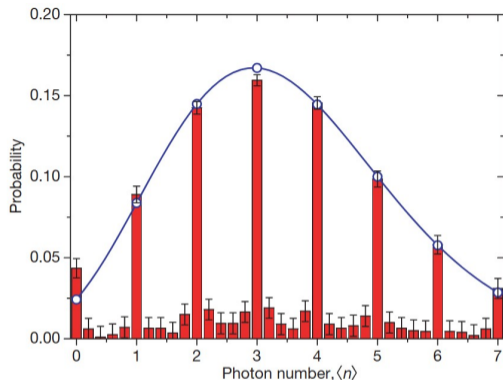


**Figure 3 | Reconstructed photon number distribution.** Histogram of  $\langle n \rangle$  values obtained from 2,000 QND collapse sequences (each involving  $N = 110$  atoms). The  $\langle n \rangle$ s are sampled in intervals of 0.2. The error bars are the statistical standard deviations. The peaks at integer numbers reveal Fock states. The background is due to incomplete or interrupted collapses. Data shown as blue circles are obtained by fitting the distribution of integer number peaks to a Poisson law, yielding  $\langle n \rangle_{\text{ave}} = 3.46 \pm 0.04$  (the blue line represents a continuous Poisson distribution joining the circles as a guide for the eye).

# Repeated measurements and field jumps

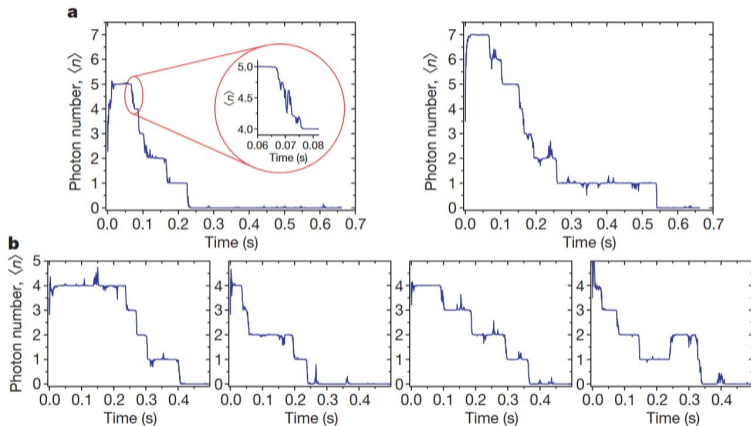


**Figure 4 | Repeated QND measurements.**

**a**, Mean photon number  $\langle n \rangle$  followed over 0.7 s for the two sequences whose collapse is analysed in Fig. 2. After converging,  $\langle n \rangle$  remains steady for a while, before successive quantum jumps bring it down to vacuum. Inset, zoom into the  $n = 5$  to 4 jump, showing that it is detected in a time of  $\sim 0.01$  s. **b**, Four other signals recording the evolution of  $\langle n \rangle$  after field collapse into  $n = 4$ . Note in the leftmost frame the exceptionally long-lived  $n = 4$  state, and in the rightmost frame the  $n = 1$  to 2 jump revealing a thermal field fluctuation.